Published in final edited form as:
Neuron. 2010 June 10; 66(5): 755–767. doi:10.1016/j.neuron.2010.04.035.

TARP phosphorylation regulates synaptic AMPA receptors through lipid bilayers

Akio Sumioka[1,2,3], **Dan Yan**[1,2,3], and **Susumu Tomita**[1,2,*]

[1] Departments of Cellular and Molecular Physiology, Yale University School of Medicine, New Haven, CT 06510

[2] Program in Cellular Neuroscience, Neurodegeneration and Repair, Yale University School of Medicine, New Haven, CT 06510

Summary

Neurons use neurotransmitters to communicate across synapses, constructing neural circuits in the brain. AMPA-type glutamate receptors are the predominant excitatory neurotransmitter receptors mediating fast synaptic transmission. AMPA receptors localize at synapses by forming protein complexes with transmembrane AMPA receptor regulatory proteins (TARPs) and PSD-95-like MAGUKs. Among the three classes of ionotropic glutamate receptors (AMPA-, NMDA, kainate-type), AMPA receptor activity is most regulatable by neuronal activity to adjust synaptic strength. Here, we mutated the prototypical TARP, stargazin, and found that TARP phosphorylation regulates synaptic AMPA receptor activity *in vivo*. We also found that stargazin interacts with negatively-charged lipid bilayers in its phosphorylation dependent manner, and that the lipid interaction inhibited stargazin binding to PSD-95. Cationic lipids dissociated stargazin from lipid bilayers and enhanced synaptic AMPA receptor activity in a stargazin phosphorylation-dependent manner. Thus, TARP phosphorylation plays a critical role in regulating AMPA receptor-mediated synaptic transmission via a lipid bilayer interaction.

Introduction

Neurons communicate at synapses through neurotransmitters, and a major excitatory neurotransmitter in the brain is glutamate. AMPA-type glutamate receptors mediate fast synaptic transmission. Among the three classes of ionotropic glutamate receptors (AMPA-, NMDA, kainate-type), AMPA receptor activity is the most highly regulated by neuronal activity, which serves adjust synaptic strength (Collingridge et al., 2004; Kessels and Malinow, 2009; Lisman, 2003; Malenka and Bear, 2004; Nelson and Turrigiano, 2008). Neuronal activity regulates synaptic strength by controlling the numbers of AMPA receptor at synapses (Collingridge et al., 2004; Kessels and Malinow, 2009; Lisman, 2003; Malenka and Bear, 2004; Nelson and Turrigiano, 2008; Newpher and Ehlers, 2008; Shepherd and Huganir, 2007).

The characteristic structure of excitatory synapses is the post-synaptic density (PSD), which is observed as an electron-dense area underlying the postsynaptic membrane. The PSD-

*To whom correspondence should be addressed @ Yale University School of Medicine, 295 Congress Avenue BCMM441, PO Box 9812, New Haven, CT 06510, Susumu.Tomita@yale.edu.

[3]These authors contributed equally to this work.

enriched prototypical PDZ protein, PSD-95, is a membrane-associated guanylate kinase (MAGUK) that contains three PDZ domains (Cho et al., 1992). Overexpression of PSD-95 in hippocampal neurons was found to drive the maturation of excitatory synapses, as evidenced by enhanced synaptic clustering and activity of AMPA receptors (El-Husseini et al., 2000). Acute knockdown of PSD-95 expression by RNAi revealed a specific loss of AMPA receptor-mediated excitatory postsynaptic currents (EPSCs) (Beique and Andrade, 2003; Elias et al., 2006; Nakagawa et al., 2004; Schluter et al., 2006). Furthermore, targeted disruption of PSD-95 in mice alters synaptic plasticity such that long term potentiation (LTP) is enhanced and long term depression (LTD) is eliminated (Migaud et al., 1998). LTP was occluded in hippocampal neurons in which PSD-95 was overexpressed (Ehrlich and Malinow, 2004; Stein et al., 2003). Importantly, although PSD-95 cannot directly interact with AMPA receptors, it nevertheless specifically enhances AMPA receptor activity.

AMPA receptors contain transmembrane AMPA receptor regulatory proteins (TARPs) as their auxiliary subunits (Coombs and Cull-Candy, 2009; Nicoll et al., 2006; Osten and Stern-Bach, 2006; Sager et al., 2009; Ziff, 2007). TARPs are classified as class I (stargazin/γ-2, γ-3, γ-4, and γ-8) and class II (γ-5 and γ-7), and are evolutionally conserved (Kato et al., 2008; Tomita et al., 2003; Wang et al., 2008). TARPs interact with AMPA receptors and modulate trafficking, channel activity and pharmacology of AMPA receptors (Chen et al., 2000; Cho et al., 2007; Kato et al., 2007; Kott et al., 2007; Menuz et al., 2007; Milstein et al., 2007; Priel et al., 2005; Soto et al., 2007; Tomita et al., 2005a; Tomita et al., 2006; Turetsky et al., 2005). Furthermore, TARPs binds to PSD-95-like MAGUKs to stabilize the AMPA receptor/TARP complex at synapses (Bats et al., 2007; Chen et al., 2000; Dakoji et al., 2003). AMPA receptor-mediated synaptic transmission is reduced in the cerebellar granule cells from stargazer mice in which the prototypical TARP stargazin/γ-2 is disrupted, and in the hippocampal pyramidal cells of TARP/γ-8 knockout mice (Hashimoto et al., 1999; Rouach et al., 2005). Furthermore, TARP triple knockout mice (γ-2/3/4, γ-2/3/8) were died after birth without moving, indicating the necessity of TARPs for postnatal survival (Menuz et al., 2009). These results indicate that AMPA receptors localize at synapses by forming protein complexes with TARPs and PSD-95-like MAGUKs. However, it remains unclear as to how neuronal activity modulates the number of AMPA receptors at synapses.

Synaptic targeting of AMPA receptors has been suggested to be regulated by TARPs (Tomita et al., 2005b; Tsui and Malenka, 2006). TARPs are highly phosphorylated at synapses and their phosphorylation is regulated bidirectionally upon neuronal activity (Inamura et al., 2006; Tomita et al., 2005b). Furthermore, neuronal synaptic AMPA receptor activity at synapses is enhanced by overexpression of a TARP mutant that mimics the phosphorylated state of TARPs (Kessels et al., 2009; Tomita et al., 2005b).

In this study, we explored the mechanisms regulating the activity of synaptic AMPA receptors and determined that TARPs interact with negatively-charged lipid bilayers in a TARP phosphorylation-mediated manner. TARP phosphorylation modulates synaptic AMPA receptor activity in vivo using TARP knockins carrying mutations in its phosphorylation sites. Interaction of lipids with TARPs inhibits TARP binding to PSD-95, which is required for synaptic localization of the AMPA receptor/TARP complex. Furthermore, cationic lipids dissociate TARPs from lipid bilayers and increase the activity of synaptic AMPA receptors in a TARP phosphorylation-dependent manner. Therefore, we conclude that the synaptic activity of AMPA receptors is controlled by TARP phosphorylation via PSD-95 binding, which is modulated by the TARP-lipid bilayer interaction.

Results

TARP phosphorylation increases AMPA receptor activity at synapses

The prototypical TARP, stargazin, at the PSD is highly phosphorylated (Tomita et al., 2005). Nine serine residues located in a short consecutive region of the stargazin cytoplasmic domain were identified previously (Tomita et al., 2005). To examine the roles played by TARP phosphorylation *in vivo*, we generated knockin mice containing mutations in the prototypical TARP, stargazin. Phosphorylated stargazin at the PSD migrated at a molecular weight that was similar to that of the stargazin^{SD} mutant, in which the nine phosphorylatable serine residues were mutagenized to aspartate (phospho-mimic mutant) (Tomita et al., 2005). To examine how many of the nine phosphorylatable serine residues in stargazin were phosphorylated at synapses, we examined the shifts in molecular weight of each stargazin mutant using SDS–PAGE (Figure S1A, B). We found that stargazin^{SD} migrated at a higher molecular weight compared with stargazin^{SA}, in a number of phosphomimic mutation-dependent manner (Figure S1A) and that no single phosphomimic mutation caused dramatic shifts in the molecular weight of stargazin^{SD} (Figure S1B). Importantly, the molecular weight of stargazin^{SD} was larger than that of three distinct stargazin mutants that carry six of phosphomimic mutations at different phosphorylatable serine residues, which suggest that the stargazin molecules located at synapses are phosphorylated at at least seven sites (Figure S1A). To examine the roles of stargazin phosphorylation, we mutated all nine phosphorylatable serine residues to aspartate (phospho-mimic, stargazin^{SD}) or alanine (non-phospho-mimic, stargazin^{SA}; Figure S1C–E). Following lambda phosphatase treatment, wild-type stargazin shifted to a lower molecular weight (Figure 1A). In contrast, the molecular weights of mutated proteins from Stargazin^{SD} and Stargazin^{SA} mice remained unchanged, and corresponded to the molecular weights for phosphorylated and non-phosphorylated stargazin, respectively (Figure 1A). These results were confirmed using three different antibodies against stargazin (Figure 1A). Both Stargazin^{SD} and Stargazin^{SA} homozygous mice are fertile and viable and did not exhibit changes in protein expression of synaptic proteins, which included stargazin, AMPA receptors (GluA1–4), NMDA receptor (GluN1), and MAGUKs (PSD-93 and -95 and SAP97 and 102) (Figure S1F). To examine how the stargazin phosphorylation state affects its distribution, we fractionated brains from wild-type mice and hemizygous Stargazin^{SD} and Stargazin^{SA} mice. Wild-type stargazin was highly phosphorylated in the PSD fraction (Tomita et al., 2005) (Figure 1B). Stargazin^{SD} fractionated predominantly into the PSD fraction, whereas stargazin^{SA} fractionated evenly into both the PSD and Triton X-100-soluble non-synaptic fractions, which indicates that the phosphorylation of stargazin modulates its synaptic distribution *in vivo* (Figure 1C).

Next we explored changes in AMPA receptor activity in cerebellar granule neurons, in which stargazin is the only TARP expressed (Chen et al., 2000; Hashimoto et al., 1999). We measured the excitatory synaptic transmission at cerebellar mossy fiber (MF)/granule cell synapses using acute cerebellar slices (Figure 2). The AMPA receptor component of excitatory postsynaptic currents (EPSCs) (I_{AMPA}) was measured as the peak amplitude at a holding potential of −70 mV, whereas the NMDA receptor component of EPSCs (I_{NMDA}) was measured at a holding potential of +40 mV and at a 50 ms latency. We did not detect an AMPA receptor component of EPSCs elicited by MF stimulation in neurons from *stargazer* mice (Figure 2A), as published previously (Hashimoto et al., 1999). The ratio of the AMPA receptor to the NMDA receptor components of EPSCs was measured among different genotypes; we found that the AMPA/NMDA receptor ratio was increased by 75% in stargazin^{SD} mice and decreased by 38 % in stargazin^{SA} mice compared with wild-type animals (Figure 2A), without changes in I–V relationships and paired-pulse facilitation (40 ms interval) (Figure 2B–D). These results strongly indicate that postsynaptic properties were altered in stargazin-phosphorylated knockin animals. To test this directly, we measured

miniature EPSCs (mEPSCs) using 1 μM tetrodotoxin (Figure 2E). We did not detect any obvious events in cerebellar granule cells from *stargazer* mice (Figure 2E). mEPSC amplitudes were significantly larger in stargazin^{SD} than in stargazin^{SA} mice and the mEPSC amplitudes detected in wild-type mice were intermediate to those observed for the two knockin mice, with a less steep cumulative probability, which suggests the presence of synaptic heterogeneity in wild-type neurons (Figure 2F). Moreover, interevent intervals (mEPSC frequency) were not different among different genotypes (Figure 2G). These results indicate that AMPA receptor activity was increased at synapses of stargazin^{SD} animals and decreased at synapses of stargazin^{SA} mice.

In addition to the evaluation of synaptic transmission in acute cerebellar slices, we also examined synaptic transmission in primary cultures of cerebellar granule cells. To avoid complexity from experimental conditions, we used a mixed population of cerebellar granule neurons from homozygous Stargazin^{SA} and Stargazin^{SD} mice on each plate. To identify genotype, either mouse carries the extra GFP transgene by mating GFP transgenic mice and stargazin knockins. We measured AMPA receptor-mediated mEPSC (Figure S2A). Neurons from Stargazin^{SD} mice exhibited significantly larger amplitudes of AMPA receptor-mediated mEPSCs than Stargazin^{SA} neurons but no significant difference in frequency or decay kinetics of mEPSCs (Figures S2B–E). These results indicate that more AMPA receptors localize at synapses of Stargazin^{SD} mice than Stargazin^{SA} mice, which is consistent with findings that were obtained using acute cerebellar slices (Figure 2). To examine AMPA receptor activity at the cell surface, we measured AMPA-evoked currents and found that neurons from stargazin^{SD} mice exhibited significantly larger AMPA-evoked currents compared with those from wild-type or stargazin^{SA} mice (Figure S2F). Whereas AMPA-evoked currents in WT and Stargazin^{SA} mice were at similar level, mEPSC amplitude in WT is larger than one in Stargazin^{SA}, indicating that Stargazin^{SA} expressed at the cell surface, but trapped outside of synapses.

Stargazin binds negatively-charged lipids in a phosphorylation-dependent manner

We next explored the mechanism underlying preferential synaptic localization of Stargazin^{SD}. A simple model might predict that a molecule interacting with stargazin in a phosphorylation-dependent manner would regulate localization of the stargazin/AMPA receptor complex. To search for such a molecule, we initially took a proteomic approach, co-purifying AMPA receptors with stargazin from both Stargazin^{SD} and Stargazin^{SA} mice (Figure S3B). However, silver staining did not detect obvious interactors with stargazin in a phosphorylation-dependent manner in detergent-soluble brain lysates (Figure S3A). Therefore, we next examined whether lipids interacted with stargazin. We purified the GST-tagged cytoplasmic domain of stargazin and overlaid it onto a membrane spotted with various lipids. Interaction with stargazin was detected with negatively-charged lipids including phosphatidic acid (PA), phosphatidylinositol-4-phosphate (PIP), phosphatidylinositol-4,5-biphosphate (PIP_2), and phosphatidylinositol-3,4-5-triphosphate (PIP_3)(Figure 3A). Interactions were observed between lipids and stargazin wild-type/ stargazin^{SA}, but not stargazin^{SD} (Figure 3A). We then examined interaction of stargazin with liposome – more native forms of lipids. Liposomes containing phosphatidylcholine (PC) alone, or with various other lipids (9:1), were mixed with the thioredoxin-tagged cytoplasmic domain of stargazin. Sucrose gradient centrifugation was used to separate liposome bound-stargazin from the unbound protein. We detected interactions between stargazin and liposomes containing negatively-charged (PIP_2, PA) or polar lipids (phosphatidylserine [PS] or phosphatidylglycerol [PG]); interactions were not observed with neutrally-charged lipids (phosphatidylethanolamine [PE] or PC; Figures 3B and C). The difference in results using polar lipids between a lipid strip assay and a liposome binding assay arose from the properties of polar lipids, in that liposomes containing polar lipids can

be negatively charged at their surface because of the directional alignment of polar lipids, whereas polar lipids aligned randomly on lipid strips are neutral. Importantly, wild-type stargazin and stargazin^{SA} bound the PA/PC liposome, whereas stargazin^{SD} did not (Figures 3D and E). Furthermore, eight positively charged amino acids (arginines) are located around the phosphorylatable serine residues in stargazin. To examine the role of positively charged residues in the interaction of stargazin with negatively charged lipid bilayers, we replaced the eight arginine residues with seven leucine and one glycine residues (RL). We found that stargazin^{RL} did not interact with negatively charged liposomes (Figure 3F). These experiments establish that stargazin interacts with a negatively-charged lipid bilayer in a phosphorylation and electrostatic-dependent manner.

Lipid bilayers inhibit binding of stargazin to PSD-95

It has been shown that the four C-terminal amino acids of stargazin bind PDZ domains of PSD-95-like MAGUKs, which scaffold signaling molecules at synapses (Bats et al., 2007; Chen et al., 2000; Dakoji et al., 2003; Schnell et al., 2002). To examine how stargazin phosphorylation affects its ability to bind to PSD-95, the cytoplasmic domain of stargazin was mixed with GST-fused PSD-95 (PDZ domains 1–3), followed by recovery of GST-fused proteins with glutathione beads to separate the PSD-95-binding fraction. Stargazin mutants lacking the last four amino acids (Δ4) did not interact with PSD-95, whereas both Stargazin^{SD} and Stargazin^{SA} interacted with PSD-95 to a similar extent (Figure 4A). Thus, stargazin phosphorylation does not affect interaction with PSD-95 in the absence of lipids.

Next, we examined the effects of lipid interaction on binding between stargazin and PSD-95. Stargazin proteins were covalently conjugated to liposomes containing 4-(p-maleimidophenyl)butyramide (MPB)-PE via the MPB-cysteine thiol-maleimide reaction, to avoid complications arising from direct interaction between stargazin^{SA} and the liposome (Figure 4B). After washing with 1 M NaCl to remove non-conjugated proteins from liposomes, stargazin-conjugated liposomes were mixed with PSD-95, followed by separation of bound and unbound PSD-95 by sucrose gradient centrifugation (Figure 4B; see detailed method in Figure S4A). Conjugated stargazin^{SD} and stargazin^{SA} could be detected following incorporation of MPB-PE into PC/PA (Figure 4C the first and second lanes). Furthermore, to reconstitute lipid composition in the brain, we performed a similar experiment using liposomes from a brain lipid extract (Figure 4C, bottom panel). PSD-95 bound stargazin^{SD} in both types of liposomes. In contrast, PSD-95 did not bind to stargazin^{SA} or to stargazin^{SD} lacking the four C-terminal amino acids (Δ4; Figure 4C). Furthermore, stargazin^{RL} conjugated to liposomes interacted with PSD-95, independently from stargazin phosphorylation and the presence of negatively charged lipids (Figure S4B), which suggests that the electrostatic interaction of stargazin with negatively charged lipid bilayers inhibited the binding of stargazin to PSD-95. Thus, lipids disrupt binding of stargazin to PSD-95 and phosphorylation of stargazin enables dissociation from lipid, which allows binding of PSD-95.

PSD-95 binding requires stargazin dissociation from lipid bilayers

Since the interaction between stargazin^{SA} and the negatively-charged lipid bilayer inhibits stargazin binding to PSD-95, the binding could be increased upon neutralization of the lipid bilayer charge to induce dissociation of stargazin from lipid bilayers. We added the cationic lipid lipofectamine (3:1 mixture of the cationic lipid DOSPA and of the neutral lipid DOPE, according to the Invitrogen website) to mixtures of stargazin-conjugated liposomes and PSD-95, and then separated stargazin-bound PSD-95 from the unbound protein (Figure 5A). Cationic lipids dramatically increased binding between PSD-95 and stargazin^{SA}, but not stargazin^{SA} Δ4 (Figure 5B). Interaction between stargazin^{SD} and PSD-95 was unaffected by addition of cationic lipids (Figure 5B). We detected a weak signal for both stargazin^{SA} Δ4

and stargazin^{SD} Δ4, at a level that was similar to that of liposomes conjugated with cysteine alone, which indicates that this weak signal is non-specific after addition of cationic lipids (Figure S5A). These results indicate that cationic lipids neutralize the negatively-charged lipid bilayer, which allows stargazin to dissociate from the liposome and bind to PSD-95.

Next, we explored the effect of cationic lipids on electrostatic interaction of stargazin with lipid bilayers. We needed to deliver cationic lipids from the extracellular solution to the inner leaflet of plasma membranes in neurons. We examined the effects of various cationic lipids on net charges of the inner leaflet of CHO cells using GFP fused basic proteins that recognizes negatively-charged lipids (GFP-R-Pre)(Yeung et al., 2008). The cationic lipids sphingosine and squalamine translocate GFP-R-pre from the plasma membrane to the cytosol as reported previously (Yeung et al., 2008; Yeung et al., 2006), whereas lipofectamine does not (Figure S5B). However, sphingosine could not be used for liposome experiments, since incorporation efficiency of sphingosine into 100 nm liposomes seems low. Thus, we used sphingosine as a cationic lipid to examine its effects on the electrostatic interaction of stargazin with lipid bilayers. Stargazin is a tetramembrane-spanning protein; as it is difficult to use full-length transmembrane proteins to evaluate the roles of its cytoplasmic domain in lipid interaction and distribution, we expressed the GFP-tagged cytoplasmic domain of stargazin containing a consensus myristoylated motif at its N terminus (myrSA), instead of the transmembrane-domain sequence, and confirmed its migration at the expected molecular weight in tracsfected CHO cells (Figure S5C). The molecular weight of wild-type stargazin was similar to that of stargazin^{SD}, which indicates that wild-type stargazin was nearly fully phosphorylated in CHO cells (Figure S5C).

The coexpression of various stargazin mutants with mCherry-tagged R-pre, which is a marker of negatively charged plasma membranes (Yeung et al., 2008; Yeung et al., 2006) revealed that myrSA was localized at the plasma membrane, together with mCherry-R-pre, whereas GFP, the cytoplasmic domain of stargazin^{SD} and wild type with myristoylated motif and GFP (myrSD and myrSTG) distributed in the cytoplasm (Figure 5C). Furthermore, addition of the cationic lipid sphingosine translocated myrSA from the plasma membrane to the cytoplasm (Figure 5D). These results indicate that the cytoplasmic domain of stargazin^{SA} interacted with the plasma membrane/lipid bilayers via electrostatic interactions.

Cationic lipids enhanced the synaptic activity of AMPA receptors in a stargazin phosphorylation-dependent manner

Next, we explored the roles of the interaction of stargazin with lipid bilayers on AMPA receptor activity in neurons. To explore the effects of stargazin dissociation from lipid bilayers on AMPA receptor activity, we prepared cerebellar granule neurons from Stargazin^{SD} and Stargazin^{SA} mice. Insertion of the cationic lipid sphingosine into neuronal plasma membranes was confirmed by the detection of the localization of fluorescent NBD-labeled sphingosine (Figure 6A). Sphingosine treatment significantly increased AMPA receptor-mediated mEPSCs frequency in all neurons to a similar extent (Figure 6B), as proposed recently that this sphingosine-mediated frequency enhancement might represent modulation of the vesicle fusion complex (Darios et al., 2009). Importantly, sphingosine increased mEPSC amplitude (Figure 6C), without changing the decay kinetics of mEPSCs in neurons from Stargazin^{SA} mice (Figure 6D). In contrast, a similar increase in amplitude was not observed in neurons from Stargazin^{SD} and wild-type mice (Figure 6C). AMPA receptor-mediated mEPSCs in wild-type neurons were not modulated by addition of cationic lipids, as we found that stargazin is highly phosphorylated in cultured neurons (Kim et al., 2010). Because we added tetrodotoxin (1 μM), AP-5 (100 μM) and picrotoxin (100 μM) to the extracellular recording solution, increase in AMPA receptor-mediated mEPSC amplitudes are mediated by AMPA receptor complex itself, but not by calcium signaling cascade or

complex neuronal activations. One concern regarding the experiments that used sphingosine is that sphingosine increased mEPSC frequency robustly (Figure 5B), as described previously (Darios et al., 2009). This robust change in mEPSC frequency might have some additional effects. Therefore, we used another cationic lipid, squalamine (Figure 6B and E). Similary, squalamine increased mEPSC amplitude in stargazin^{SA} neurons, but not in stargazin^{SD} and wild-type neurons. The mEPSC amplitude in stargazin^{SA} in the presence of squalamine was similar to that in stargazin^{SD}. Therefore, we concluded that cationic lipids consistently increased the mEPSC amplitude in stargazin^{SA} neurons, but not in stargazin^{SD} neurons. Next, we measured AMPA-evoked currents to monitor total AMPA receptor activity at the cell surface and found that the AMPA-evoked currents before and after treatment with cationic lipids were not different in neurons from stargazin^{SA} and stargazin^{SD} mice, which suggests that the increase in synaptic AMPA receptor activity was diffused laterally at the cell surface (Figure 6F).

As AMPA receptor activity is dependent on the level of stargazin in cerebellar granule cells, we measured changes in expression of stargazin at the PSD. We treated neurons with sphingosine and fractionated synaptic and non-synaptic proteins. We found that stargazin^{SA} was upregulated in the PSD fraction, whereas stargazin^{SD} was not (Figure 7A and B). Because the synaptic localization of stargazin requires its interaction with PSD-95, we measured the interaction of PSD-95 with stargazin after addition of the cationic lipid using coimmunoprecipitation experiments. However, solubilization of PSD-95 from neurons requires the use of a strong detergent, such as 1% SDS, which breaks the interaction of PSD-95 with stargazin. Therefore, we used a chemical crosslinker to detect the interaction of PSD-95 with stargazin. We added a crosslinker (DSP) to cerebellar granule cells treated with or without sphingosine. Solubilized proteins were subjected to immunoprecipitation with anti-stargazin antibody. To avoid an artificial interaction of stargazin with PSD-95 during incubation, we added 100 μM of a 10-mer peptide from the C terminus of stargazin (NTANRRTTPV), which allowed the *in vivo* detection of crosslinked complexes exclusively. We detected protein complexes exclusively in neurons (and not in test tubes) (Figure 7C). Furthermore, we found that sphingosine treatment increased the interaction of PSD-95 with Stargazin^{SA}, but not with Stargazin^{SD}, without changes in the total levels of protein expression (Figure 7D and E). These results indicate that the electrostatic interaction between stargazin and the negatively-charged lipid bilayers inhibits interaction between stargazin and PSD-95, and that dissociation of stargazin from the lipid bilayer increases AMPA receptor activity at synapses via lateral diffusion and interaction with PSD-95 (Figure 7F).

Discussion

The results of this study demonstrate that stargazin phosphorylation regulates synaptic AMPA receptor activity *in vivo*, using stargazin knockin mice in which the phosphorylatable serine residues were mutated to aspartate (phospho-mimic) or alanine (non-phospho-mimic) residues. Stargazin interacts with the negatively-charged lipid bilayer in a phosphorylation-dependent manner. This lipid-stargazin interaction inhibits the binding of stargazin to PSD-95. Cationic lipids dissociate stargazin from lipid bilayers and enhance the activity of synaptic AMPA receptors in a stargazin phosphorylation-dependent manner. These findings establish that negatively-charged lipid bilayers and stargazin phosphorylation are critical modulators for synaptic AMPA receptor activity.

Roles of multiple phosphorylation sites in TARPs

Stargazin has nine phosphorylated serine residues (Tomita et al., 2005b), and these phosphorylation sites are well conserved among class I TARPs (stargazin/γ-2, γ-3, γ-4 and γ-8). Indeed, γ-3 is phosphorylated at sites that correspond well to the sites of stargazin in

neurons (Tomita et al., 2005b). In this study, we mutated all nine phosphorylated serine residues either to aspartic acid as a phospho-mimic stargazin or to alanine as a non-phospho mimic stargazin, and found that stargazin interacted with negatively-charged lipid bilayers in a phosphorylation-dependent manner (Figure 3). These nine phosphorylated residues surround eight of the basic arginine residues, which recognize negative charges on lipid bilayers. Therefore, acidic phosphorylated residues inhibit interactions between the basic arginine residues in stargazin and the negatively-charged lipid bilayers. Because stargazin recognizes lipid bilayers by electrostatic interactions, the stargazin interaction with lipid bilayers is likely to depend on the number of stargazin phosphorylated residues to be graded manner, instead of binary on-off manner. Because the dissociation of stargazin from lipid bilayers enhanced the binding of stargazin to PSD-95 (Figures 4 and 5), graded interactions between stargazin and lipid bilayers could induce graded interactions between stargazin and PSD-95, which could lead to graded synaptic transmission. Graded interactions between stargazin and lipid bilayers may serve as a “molecular rheostat” and provide neurons with more dynamic synaptic transmission capabilities.

The mechanisms underlying the synaptic targeting of non-phosphorylated TARPs

In this study, we found that phosphorylated stargazin preferentially localized at synapses (Figure 1). Whereas disruption of stargazin expression in Stargazer mice resulted in no discernible AMPA receptor activity from the cerebellar granule cells, neurons of non-phosphorylated stargazin knockins had detectable synaptic AMPA receptor activity, indicating that non-phosphorylated stargazin could localize at synapses with AMPA receptors. The stargazin-AMPA receptor complex localized to synapses through PSD-95 binding, and lipid bilayers inhibited stargazin binding to PSD-95, suggesting that non-phosphorylated stargazin somehow did not interact with lipid bilayers. A possible molecular mechanism to explain these phenomena is that an unidentified molecule may bind to the non-phosphorylated form of the TARPs at synapses, and this interaction may dissociate TARPs from the lipid bilayers, leading to TARP binding with PSD-95. Another possible mechanism could be that the interaction between TARPs and lipid bilayers is weaker than the interaction between TARPs and PSD-95. Therefore, once bound to PSD-95 at synapses, the TARPs are difficult to dissociate. Characterization of the lipid composition at synapses is required for further investigation of these alternatives.

There are 64 amino acids (aa) between the most C-terminal phosphrylation site among nine phosphorylated residues and the C-terminal PDZ domain-binding motif (-TTPV). It remains unclear how stargazin phosphorylation affects the PDZ binding at the 64 amino acids away. We currently considered two possibilities. A, Schnell et al. showed that the point mutation in the second PDZ domain of PSD-95 is sufficient to block interaction with stargazin (Schnell et al., 2002). Since the second PDZ domain of PSD-95 locates at the position of 161–243 aa, 64 aa from stargazin is not enough to reach its binding pocket and dissociation of stargazin phosphorylation sites from lipid bilayers is necessary for its binding to PSD-95. B, 64 aa takes fully compacted structure and not enough distance to interact with endogenous PSD-95. To fully answer these possibilities, crystal structure at the atomic level is required.

Lipid bilayers as novel regulators of PDZ domain binding

In addition to identifying the molecular machinery that modulates AMPA receptor activity, the results of this study establish lipids as novel regulators of the interactions between PDZ domains and the PDZ domain-binding motif. The lipid composition of the inner leaflet of plasma membranes is regulated by various enzymes (Di Paolo and De Camilli, 2006), and changes in lipid composition could affect the TARP/MAGUKs interaction. In the human genome, 96 proteins contain PDZ domains and many proteins have the consensus PDZ domain-binding motif (Venter et al., 2001), suggesting that numerous combinations between

the PDZ domains and possible binding partners may exist. However, PDZ interactions appear to be tightly regulated *in vivo*. Whereas stargazin contains a typical class I PDZ-binding motif, it does not constitutively bind to PDZ proteins outside of synapses (Fukata et al., 2005; Vandenberghe et al., 2005). We propose that the lipid bilayer functions as a regulator for controlling the PDZ domain and its binding motif, and our findings provide a novel mechanism for the regulation of PDZ domain interactions.

Contribution of lipid bilayers to synaptic AMPA receptor activity

We propose that negatively-charged lipid bilayers function as modulators of AMPA receptor activity at synapses. Inositol phospholipids are some of the best-characterized negatively-charged lipids, and they strongly interact with stargazin (Figure 3C). Inositol phospholipids are modulated by various phosphatases and kinases; the metabolites contain a specific number of phosphates and are charged negatively (Di Paolo and De Camilli, 2006). Because stargazin recognizes negative charges on lipid bilayers, rapid modulation of lipid composition in the inner leaflet of plasma membranes could regulate the distribution of synaptic AMPA receptors through TARPs. Indeed, we showed here that the addition of cationic lipids increased AMPA receptor-mediated EPSCs in a TARP phosphorylation-dependent manner. Therefore, relocation of polar- lipids (PS, PG) or negatively-charged-lipids to the plasma membrane, or metabolism of phosphates on lipids could modulate the activity of synaptic AMPA receptors. Lipid composition of the plasma membranes at synapses and modulation of the lipid composition may reveal novel mechanisms for regulating the AMPA receptors at synapses. Further investigation of the lipid composition at synapses, PSDs, spines, and dendrites is required.

We found that the mini amplitude and I_{AMPA}/I_{NMDA} ratio in stargazin^{SD} mice were 1.25X and 3X the level of that in stargazin^{SA} mice, respectively (Fig 2F and A). In addition, we observed larger AMPA evoked currents in stargazin^{SD} (Fig. S2F). Because overexpression of stargazin^{WT}, ^{SA} and ^{SD} increased surface AMPA receptor activity to the similar level in neurons (Tomita et al, 2005), one possible mechanism for the enhancement of AMPA evoked currents in Stargazin^{SD} is that all stargazin might traffic to the cell surface at the similar level, but stargazin^{SD} overflowed from synapses and floating on the surface, or stargazin^{SD} mutation is escaped from protein degradation pathways.

It has been shown that PICK1 interacts with lipids via the BAR domain and the PDZ domain, independently (Jin et al., 2006; Pan et al., 2007; Steinberg et al., 2006). Furthermore, overexpression of PICK1 mutants that disrupt lipid interaction modulates the surface expression of AMPA receptors. Because we did not observe any changes in total AMPA receptor activity at the cell surface, as assessed by AMPA-evoked currents after addition of cationic lipids, the effects of cationic lipids on synaptic AMPA receptor activity seem to be independent from PICK1. The interaction of PICK1 with lipids may play a role in other brain regions.

TARP phosphorylation in synaptic plasticity

Neuronal activity modulates synaptic strength, and Hebbian or non-Hebbian types of synaptic plasticity have been established, including LTP, LTD, and synaptic scaling (Collingridge et al., 2004; Kessels and Malinow, 2009; Lisman, 2003; Malenka and Bear, 2004; Nelson and Turrigiano, 2008). The molecular mechanisms underlying these types of synaptic plasticity have been extensively studied but the substrates of synaptic plasticity have not been fully understood. Several studies of synaptic plasticity in gene-targeting mice have suggested that the AMPA receptor itself may serve as a phosphorylated substrate in distinct forms of plasticity (Lee et al., 2003). However, mice in which each subunit of the AMPA receptor is disrupted also show synaptic plasticity, suggesting that there may be

other substrates of plasticity outside of the AMPA receptor itself. TARPs may be a reasonable candidate as a substrate for synaptic plasticity because TARP phosphorylation is regulated upon neuronal activity (Tomita et al., 2005b) and TARP phosphorylation induces TARP binding to PSD-95. To directly examine this possibility, analysis of synaptic plasticity in mice carrying mutations in the TARP phosphorylation sites is required. Here, we mutated stargazin as a representative TARP in order to evaluate the roles of TARP in basal synaptic transmission because loss of stargazin disrupts the activity of synaptic AMPA receptors of cerebellar granule cells—the purest system available for evaluating TARP functions at synapses (Chen et al., 2000; Hashimoto et al., 1999). However, cerebellar granule cells are not an appropriate system for studying synaptic plasticity; hippocampal pyramidal cells may be more useful. Indeed, LTP was reduced by 75% in mice in which TARP/γ-8, a hippocampus-abundant TARP isoform, was knocked out (Rouach et al., 2005). Therefore, TARP/γ-8 knockin mice, which carry mutations in the phosphorylation sites of TARP/γ-8, are needed in order to study the roles of TARP phosphorylation in synaptic plasticity.

Experimental Procedures

Antibodies

Rabbit polyclonal antibodies were used against the following proteins: GluA1, GluA2/3, GluA4 and Pan-TARP (Millipore); TTPV and stargazin (Tomita et al., 2003); and thioredoxin (Sigma). Polyclonal antisera to GST were affinity-purified on agarose columns containing the GST proteins. Mouse monoclonal antibodies were used against PSD-95 (ABR), synaptophysin, GST (Sigma), PSD-95, PSD-93, SAP97, and SAP102 (NeuroMab).

Protein-lipid overlay assay

Membrane lipid strips (Echelon) were used for the protein overlay assay. After blocking, the membrane strips were incubated with GST-fused proteins, followed by western blotting with anti-GST antibody.

Preparation of liposomes

All synthetic lipids were purchased from Avanti Polar Lipids. Brain lipid was purchased from Sigma. Lipids were dissolved in chloroform and evaporated using argon gas in order to prepare a lipid film. The lipid film was dissolved in TE buffer, freeze-thawed, and passed though a 100 nm polycarbonate membrane using a mini-extruder (Avanti polar lipids). Liposome size was confirmed by light scattering.

Liposome-protein interaction assay

Liposomes and purified recombinant proteins were incubated in TBSE buffer (10 mM Tris pH 7.4, 150 mM NaCl, 1 mM EDTA). Liposome-protein mixtures were adjusted to 1.2 M sucrose/TBSE by adding 2 M sucrose/TBSE, and were then overlaid with 0.9 M sucrose/TBSE and 0 M sucrose/TBSE. Sucrose gradients were subjected to ultracentrifugation and the interphase between the 0 M and 0.9 M sucrose layers, and the phase containing 1.2 M sucrose layer, were recovered as “Bound” and “Unbound”, respectively.

Protein conjugation to liposomes

For the covalent conjugation of recombinant proteins, liposomes were prepared with 5% MPB-PE (Avanti polar lipids) and incubated with recombinant stargazin proteins. Free MPB was blocked with cysteine and then the protein/MPB liposome mixtures were subjected to sucrose gradient centrifugation with 1 M NaCl to remove unconjugated proteins from the liposome. The upper liposome fraction was collected and subject to ultracentrifugation at

100,000 g. The pellet was resuspended in TBSE as a liposome with covalently-conjugated protein. To control the conjugation site of stargazin proteins, we introduced an extra cysteine residue between the thrombin cleavage site and the cytoplasmic domain of stargazin. In addition, we substituted a serine for the cysteine at position 302 in order to avoid MPB-cysteine conjugation within the stargazin cytoplasmic domain, i.e., only one cysteine residue was present in the recombinant stargazin cytoplasmic domain. A cysteine residue at position 302 in the cytoplasmic domain of stargazin is not involved in AMPA receptor activity at synapses (Figure S4C and D). Proteins purified from *E. coli* were cleaved with thrombin and the resulting His6-thioredoxin products were absorbed with Ni-agarose (Qiagen) to purify the non-tagged cytoplasmic domains of stargazin.

Whole-cell recording from cerebellar slices

Sagittal cerebellar slices with a thickness of 200 μm were prepared from *stargazer*, stargazin knockin, and wild-type mice (P21–30). Patch-clamp recordings from granule cells that were identified visually in cerebellar slices were performed as described previously (Hashimoto et al., 1999). The resistance of patch pipettes was 5–10 MΩ when filled with an intracellular solution composed of (in mM): 130 caesium methanesulfonate, 5 HEPES, 5 Mg-ATP, 0.2 Na-GTP, 20 TEA, and 5 EGTA (pH 7.3, adjusted with CsOH). The composition of the standard bathing solution was (in mM): 125 NaCl, 2.4 KCl, 2 $CaCl_2$, 1 $MgCl_2$, 1.2 NaH_2PO_4, 25 $NaHCO_3$, and 25 glucose; this solution was bubbled continuously with a mixture of 95% O_2 and 5% CO_2. Bicuculline (10 μM) and picrotoxin (100 μM) were always present in the saline solution, to block spontaneous IPSCs. Stimulation and on-line data acquisition were performed using the Clampex program (version 10.2, Axon Instruments). Signals were filtered at 3 kHz and digitized at 20 kHz. For stimulation of mossy fibers in the cerebellum, the stimuli were delivered through a glass pipette with a tip of 5–10 μm in diameter that was filled with standard saline solution. Paired-pulse facilitation was performed via the delivery of two stimuli at an interval of 40 ms. Square pulses (duration, 0.1 ms; amplitude, 5 V) were applied using a World Precision Instruments A365 constant current stimulator, for focal stimulation. All recordings were performed at room temperature. mEPSC amplitude and inter-event interval from each cell was averaged. Subsequently, the average mEPSC amplitude and inter-event interval from each cell was used for statistical analysis comparing mEPSCs from each genotypes. Both T-test and ANOVA followed by Tukey's test were used; cumulative distribution was compared by Kolmogorov-Smirnov test.

Membrane interaction assay via protein localization

The GFP-R-pre and mCherry- R-pre constructs were generated using a standard PCR method with the following synthetic oligonucleotides: 5′–TACCTCGAGGAAGGATGGCCAGAGATGGTCGGCGCAGGAGACGGCGCG–3′) and (5′–TACGGATCCTTACATAATTACACATCTGGCCCTAGCGCGCCGTCTCCT–3′). myrSTG-GFP, myrSA-GFP, and myrSD-GFP were generated using a PCR method with primers containing the myristoylation consensus sequence of MARCKs (Towler et al., 1988). CHO cells were plated onto poly-D-lysine-coated LAB-TEK 4-well chambered coverglass (Nunc). After 16–18 h of transfection, cells were observed using a Zeiss LSM510 Meta confocal microscope.

Supplementary Material

Refer to Web version on PubMed Central for supplementary material.

Acknowledgments

The authors would like to thank members of the Tomita lab, Pietro De Camilli and David McCormick for thoughtful discussions, Masanobu Kano for technical advice, and David Bredt for critical reading. We thank the Yale transgenic facility for help with the gene targeting mice, Yale/NIDA neuroproteomics Center supported by P30DA018343 for their support, and Fred Sigworth and David Chester for their dynamic light scattering system and thoughtful discussions. We thank Roger Tsien (UCSD) for providing the mCherry cDNA and Michael Zasloff (Georgetown University Medical Center) for providing squalamine. The monoclonal antibodies were obtained from the UC Davis/NIH NeuroMab Facility. S.T. is supported by NIH (MH077939), Alfred P. Sloan research fellowship, NARSAD young investigator award, Esther A. & Joseph Klingenstein Fund and Edward Mallinckrodt Jr. Foundation. A.S. is supported by JSPS.

References

Bats C, Groc L, Choquet D. The interaction between Stargazin and PSD-95 regulates AMPA receptor surface trafficking. Neuron. 2007; 53:719–734. [PubMed: 17329211]

Beique JC, Andrade R. PSD-95 regulates synaptic transmission and plasticity in rat cerebral cortex. J Physiol. 2003; 546:859–867. [PubMed: 12563010]

Chen L, Chetkovich DM, Petralia RS, Sweeney NT, Kawasaki Y, Wenthold RJ, Bredt DS, Nicoll RA. Stargazin regulates synaptic targeting of AMPA receptors by two distinct mechanisms. Nature. 2000; 408:936–943. [PubMed: 11140673]

Cho CH, St-Gelais F, Zhang W, Tomita S, Howe JR. Two Families of TARP Isoforms that Have Distinct Effects on the Kinetic Properties of AMPA Receptors and Synaptic Currents. Neuron. 2007; 55:890–904. [PubMed: 17880893]

Cho KO, Hunt CA, Kennedy MB. The rat brain postsynaptic density fraction contains a homolog of the Drosophila discs-large tumor suppressor protein. Neuron. 1992; 9:929–942. [PubMed: 1419001]

Collingridge GL, Isaac JT, Wang YT. Receptor trafficking and synaptic plasticity. Nat Rev Neurosci. 2004; 5:952–962. [PubMed: 15550950]

Coombs ID, Cull-Candy SG. Transmembrane AMPA receptor regulatory proteins and AMPA receptor function in the cerebellum. Neuroscience. 2009; 162:656–665. [PubMed: 19185052]

Dakoji S, Tomita S, Karimzadegan S, Nicoll RA, Bredt DS. Interaction of transmembrane AMPA receptor regulatory proteins with multiple membrane associated guanylate kinases. Neuropharmacology. 2003; 45:849–856. [PubMed: 14529722]

Darios F, Wasser C, Shakirzyanova A, Giniatullin A, Goodman K, Munoz-Bravo JL, Raingo J, Jorgacevski J, Kreft M, Zorec R, et al. Sphingosine facilitates SNARE complex assembly and activates synaptic vesicle exocytosis. Neuron. 2009; 62:683–694. [PubMed: 19524527]

Di Paolo G, De Camilli P. Phosphoinositides in cell regulation and membrane dynamics. Nature. 2006; 443:651–657. [PubMed: 17035995]

Ehrlich I, Malinow R. Postsynaptic density 95 controls AMPA receptor incorporation during long-term potentiation and experience-driven synaptic plasticity. J Neurosci. 2004; 24:916–927. [PubMed: 14749436]

El-Husseini AE, Schnell E, Chetkovich DM, Nicoll RA, Bredt DS. PSD-95 involvement in maturation of excitatory synapses. Science. 2000; 290:1364–1368. [PubMed: 11082065]

Elias GM, Funke L, Stein V, Grant SG, Bredt DS, Nicoll RA. Synapse-Specific and Developmentally Regulated Targeting of AMPA Receptors by a Family of MAGUK Scaffolding Proteins. Neuron. 2006; 52:307–320. [PubMed: 17046693]

Fukata Y, Tzingounis AV, Trinidad JC, Fukata M, Burlingame AL, Nicoll RA, Bredt DS. Molecular constituents of neuronal AMPA receptors. J Cell Biol. 2005; 169:399–404. [PubMed: 15883194]

Hashimoto K, Fukaya M, Qiao X, Sakimura K, Watanabe M, Kano M. Impairment of AMPA receptor function in cerebellar granule cells of ataxic mutant mouse stargazer. J Neurosci. 1999; 19:6027–6036. [PubMed: 10407040]

Inamura M, Itakura M, Okamoto H, Hoka S, Mizoguchi A, Fukazawa Y, Shigemoto R, Yamamori S, Takahashi M. Differential localization and regulation of stargazin-like protein, gamma-8 and stargazin in the plasma membrane of hippocampal and cortical neurons. Neurosci Res. 2006; 55:45–53. [PubMed: 16516319]

Jin W, Ge WP, Xu J, Cao M, Peng L, Yung W, Liao D, Duan S, Zhang M, Xia J. Lipid binding regulates synaptic targeting of PICK1, AMPA receptor trafficking, and synaptic plasticity. J Neurosci. 2006; 26:2380–2390. [PubMed: 16510715]

Kato AS, Siuda ER, Nisenbaum ES, Bredt DS. AMPA receptor subunit-specific regulation by a distinct family of type II TARPs. Neuron. 2008; 59:986–996. [PubMed: 18817736]

Kato AS, Zhou W, Milstein AD, Knierman MD, Siuda ER, Dotzlaf JE, Yu H, Hale JE, Nisenbaum ES, Nicoll RA, et al. New transmembrane AMPA receptor regulatory protein isoform, gamma-7, differentially regulates AMPA receptors. J Neurosci. 2007; 27:4969–4977. [PubMed: 17475805]

Kessels HW, Kopec CD, Klein ME, Malinow R. Roles of stargazin and phosphorylation in the control of AMPA receptor subcellular distribution. Nat Neurosci. 2009; 12:888–896. [PubMed: 19543281]

Kessels HW, Malinow R. Synaptic AMPA receptor plasticity and behavior. Neuron. 2009; 61:340–350. [PubMed: 19217372]

Kim KS, Yan D, Tomita S. Assembly and stoichiometry of the AMPA receptor and transmembrane AMPA receptor regulatory protein complex. J Neurosci. 2010; 30:1064–1072. [PubMed: 20089915]

Kott S, Werner M, Korber C, Hollmann M. Electrophysiological properties of AMPA receptors are differentially modulated depending on the associated member of the TARP family. J Neurosci. 2007; 27:3780–3789. [PubMed: 17409242]

Lee HK, Takamiya K, Han JS, Man H, Kim CH, Rumbaugh G, Yu S, Ding L, He C, Petralia RS, et al. Phosphorylation of the AMPA receptor GluR1 subunit is required for synaptic plasticity and retention of spatial memory. Cell. 2003; 112:631–643. [PubMed: 12628184]

Lisman J. Long-term potentiation: outstanding questions and attempted synthesis. Philos Trans R Soc Lond B Biol Sci. 2003; 358:829–842. [PubMed: 12740130]

Malenka RC, Bear MF. LTP and LTD: an embarrassment of riches. Neuron. 2004; 44:5–21. [PubMed: 15450156]

Menuz K, Kerchner GA, O'Brien JL, Nicoll RA. Critical role for TARPs in early development despite broad functional redundancy. Neuropharmacology. 2009; 56:22–29. [PubMed: 18634809]

Menuz K, Stroud RM, Nicoll RA, Hays FA. TARP Auxiliary Subunits Switch AMPA Receptor Antagonists into Partial Agonists. Science. 2007; 318:815–817. [PubMed: 17975069]

Migaud M, Charlesworth P, Dempster M, Webster LC, Watabe AM, Makhinson M, He Y, Ramsay MF, Morris RG, Morrison JH, et al. Enhanced long-term potentiation and impaired learning in mice with mutant postsynaptic density-95 protein. Nature. 1998; 396:433–439. [PubMed: 9853749]

Milstein AD, Zhou W, Karimzadegan S, Bredt DS, Nicoll RA. TARP Subtypes Differentially and Dose-Dependently Control Synaptic AMPA Receptor Gating. Neuron. 2007; 55:905–918. [PubMed: 17880894]

Nakagawa T, Futai K, Lashuel HA, Lo I, Okamoto K, Walz T, Hayashi Y, Sheng M. Quaternary structure, protein dynamics, and synaptic function of SAP97 controlled by L27 domain interactions. Neuron. 2004; 44:453–467. [PubMed: 15504326]

Nelson SB, Turrigiano GG. Strength through diversity. Neuron. 2008; 60:477–482. [PubMed: 18995822]

Newpher TM, Ehlers MD. Glutamate receptor dynamics in dendritic microdomains. Neuron. 2008; 58:472–497. [PubMed: 18498731]

Nicoll RA, Tomita S, Bredt DS. Auxiliary subunits assist AMPA-type glutamate receptors. Science. 2006; 311:1253–1256. [PubMed: 16513974]

Osten P, Stern-Bach Y. Learning from stargazin: the mouse, the phenotype and the unexpected. Curr Opin Neurobiol. 2006; 16:275–280. [PubMed: 16678401]

Pan L, Wu H, Shen C, Shi Y, Jin W, Xia J, Zhang M. Clustering and synaptic targeting of PICK1 requires direct interaction between the PDZ domain and lipid membranes. EMBO J. 2007; 26:4576–4587. [PubMed: 17914463]

Priel A, Kolleker A, Ayalon G, Gillor M, Osten P, Stern-Bach Y. Stargazin reduces desensitization and slows deactivation of the AMPA-type glutamate receptors. J Neurosci. 2005; 25:2682–2686. [PubMed: 15758178]

Rouach N, Byrd K, Petralia RS, Elias GM, Adesnik H, Tomita S, Karimzadegan S, Kealey C, Bredt DS, Nicoll RA. TARP gamma-8 controls hippocampal AMPA receptor number, distribution and synaptic plasticity. Nat Neurosci. 2005; 8:1525–1533. [PubMed: 16222232]

Sager C, Tapken D, Kott S, Hollmann M. Functional modulation of AMPA receptors by transmembrane AMPA receptor regulatory proteins. Neuroscience. 2009; 158:45–54. [PubMed: 18304745]

Schluter OM, Xu W, Malenka RC. Alternative N-terminal domains of PSD-95 and SAP97 govern activity-dependent regulation of synaptic AMPA receptor function. Neuron. 2006; 51:99–111. [PubMed: 16815335]

Schnell E, Sizemore M, Karimzadegan S, Chen L, Bredt DS, Nicoll RA. Direct interactions between PSD-95 and stargazin control synaptic AMPA receptor number. Proc Natl Acad Sci U S A. 2002; 99:13902–13907. [PubMed: 12359873]

Shepherd JD, Huganir RL. The Cell Biology of Synaptic Plasticity: AMPA Receptor Trafficking. Annu Rev Cell Dev Biol. 2007

Soto D, Coombs ID, Kelly L, Farrant M, Cull-Candy SG. Stargazin attenuates intracellular polyamine block of calcium-permeable AMPA receptors. Nat Neurosci. 2007; 10:1260–1267. [PubMed: 17873873]

Stein V, House DR, Bredt DS, Nicoll RA. Postsynaptic density-95 mimics and occludes hippocampal long-term potentiation and enhances long-term depression. J Neurosci. 2003; 23:5503–5506. [PubMed: 12843250]

Steinberg JP, Takamiya K, Shen Y, Xia J, Rubio ME, Yu S, Jin W, Thomas GM, Linden DJ, Huganir RL. Targeted in vivo mutations of the AMPA receptor subunit GluR2 and its interacting protein PICK1 eliminate cerebellar long-term depression. Neuron. 2006; 49:845–860. [PubMed: 16543133]

Tomita S, Adesnik H, Sekiguchi M, Zhang W, Wada K, Howe JR, Nicoll RA, Bredt DS. Stargazin modulates AMPA receptor gating and trafficking by distinct domains. Nature. 2005a; 435:1052–1058. [PubMed: 15858532]

Tomita S, Chen L, Kawasaki Y, Petralia RS, Wenthold RJ, Nicoll RA, Bredt DS. Functional studies and distribution define a family of transmembrane AMPA receptor regulatory proteins. J Cell Biol. 2003; 161:805–816. [PubMed: 12771129]

Tomita S, Sekiguchi M, Wada K, Nicoll RA, Bredt DS. Stargazin controls the pharmacology of AMPA receptor potentiators. Proc Natl Acad Sci U S A. 2006; 103:10064–10067. [PubMed: 16785437]

Tomita S, Stein V, Stocker TJ, Nicoll RA, Bredt DS. Bidirectional synaptic plasticity regulated by phosphorylation of stargazin-like TARPs. Neuron. 2005b; 45:269–277. [PubMed: 15664178]

Towler DA, Gordon JI, Adams SP, Glaser L. The biology and enzymology of eukaryotic protein acylation. Annu Rev Biochem. 1988; 57:69–99. [PubMed: 3052287]

Tsui J, Malenka RC. Substrate localization creates specificity in calcium/calmodulin-dependent protein kinase II signaling at synapses. J Biol Chem. 2006; 281:13794–13804. [PubMed: 16551613]

Turetsky D, Garringer E, Patneau DK. Stargazin modulates native AMPA receptor functional properties by two distinct mechanisms. J Neurosci. 2005; 25:7438–7448. [PubMed: 16093395]

Vandenberghe W, Nicoll RA, Bredt DS. Stargazin is an AMPA receptor auxiliary subunit. Proc Natl Acad Sci U S A. 2005; 102:485–490. [PubMed: 15630087]

Venter JC, Adams MD, Myers EW, Li PW, Mural RJ, Sutton GG, Smith HO, Yandell M, Evans CA, Holt RA, et al. The sequence of the human genome. Science. 2001; 291:1304–1351. [PubMed: 11181995]

Wang R, Walker CS, Brockie PJ, Francis MM, Mellem JE, Madsen DM, Maricq AV. Evolutionary conserved role for TARPs in the gating of glutamate receptors and tuning of synaptic function. Neuron. 2008; 59:997–1008. [PubMed: 18817737]

Yeung T, Gilbert GE, Shi J, Silvius J, Kapus A, Grinstein S. Membrane phosphatidylserine regulates surface charge and protein localization. Science. 2008; 319:210–213. [PubMed: 18187657]

Yeung T, Terebiznik M, Yu L, Silvius J, Abidi WM, Philips M, Levine T, Kapus A, Grinstein S. Receptor activation alters inner surface potential during phagocytosis. Science. 2006; 313:347–351. [PubMed: 16857939]

Ziff EB. TARPs and the AMPA receptor trafficking paradox. Neuron. 2007; 53:627–633. [PubMed: 17329203]

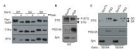

Figure 1. Stargazin phosphorylation regulates synaptic localization of stargazin

All nine phosphorylated serine residues of stargazin (STG) were mutated to either aspartate (phospho-mimic; stargazin^{SD}) or alanine (non-phospho mimic; stargazin^{SA}) in knockin mice. (A) Lambda phosphatase treatment (PPase) lowered the molecular weight of stargazin from wild-type mice (WT), but not from Stargazin^{SD} (SD) or Stargazin^{SA} mice (SA). Western blots performed with three different anti-stargazin antibodies showed similar patterns. Western blots of fractionated brains from WT (B), and Stargazin^{SD}/Stargazin^{SA} hemizygous mice (C) showed that stargazin in synaptic fraction (PSD) migrated as higher molecular weight than that in non-synaptic fraction (Syn/Tx) (B). (C) Stargazin^{SD} was highly enriched in the postsynaptic density (PSD) fraction, whereas stargazin^{SA} was distributed evenly between the PSD and Triton-X-100-soluble synaptosome (Syn/Tx) fractions. Sph, synaptophysin. Geno, genotype.

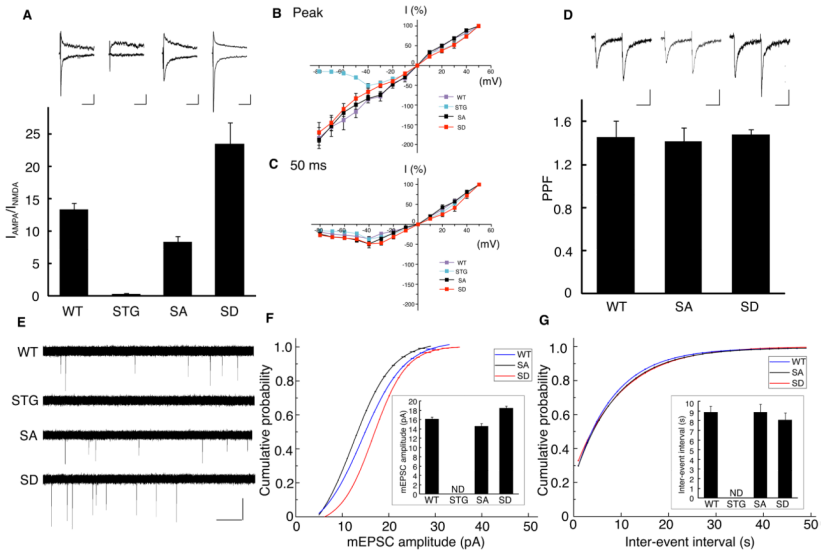

Figure 2. Stargazin phosphorylation modulates AMPA receptor activity in cerebellar mossy fiber/granule cell synapses *in vivo*

(A) EPSCs elicited by mossy fiber stimulation were recorded in cerebellar granule cells from wild-type (WT), *stargazer* (STG), and stargazin knockin mice (SA and SD). The AMPA receptor component of EPSCs (I_{AMPA}) was measured as the peak amplitude at a holding potential of −70 mV and the NMDA receptor component (I_{NMDA}) was measured at a holding potential of +40 mV and at 50 ms latency. The ratio of I_{AMPA} to I_{NMDA} was increased by ~75% in stargazin^{SD} mice compared with wild-type mice ($P < 0.01$; n = 6 for wild-type mice and n = 7 for stargazin^{SD} mice), and reduced by ~38% in stargazin^{SA} mice compared with wild-type mice ($P < 0.01$; n = 6 for wild-type mice and n = 6 for stargazin^{SA} mice). The I_{AMPA} was invisible in stargazer mice (n = 6). Sample traces of EPSCs are shown in A at a holding potential of −70 mV (bottom) or +40 mV (top). Scale bar, 20 ms and 40 pA (WT), 10 pA (STG), 20 pA (SA), and 50 pA (SD). (B, C) I–V relationships of MF–EPSCs from each genotype, measured at the peak of (B), and 50 ms (C) after, the stimulus. The EPSC amplitudes were normalized to the mean value at +50 mV in each genotype (n = 6–7). (D) Paired-pulse facilitation (PPF) values measured at 40 ms intervals did not differ among the genotypes (n = 6–7). (E, F, and G) mEPSCs recorded from cerebellar granule cells in acute cerebellar slices at a holding potential of −70 mV in the presence of 1 μM TTX. Sample traces are shown in (E). (F) Cumulative distribution of mEPSC amplitudes and average mEPSC amplitude (small inset). The mEPSC amplitude was significantly larger in stargazin^{SD} mice compared with wild-type mice ($P < 0.01$, Kolmogorov–Smirnov test for cumulative distribution; $P < 0.01$, one-way ANOVA for average, n = 10 for wild-type mice and n = 11 for stargazin^{SD} mice), whereas it was significantly smaller in stargazin^{SA} mice compared with wild-type mice ($P < 0.01$, Kolmogorov–Smirnov test for cumulative distribution; $P < 0.05$, one-way ANOVA for average, n = 10 for wild-type mice and n = 9 for stargazin^{SA} mice). However, the time intervals between events (G) were not significantly different among the genotypes. Error bars in all graphs represent the SEM.

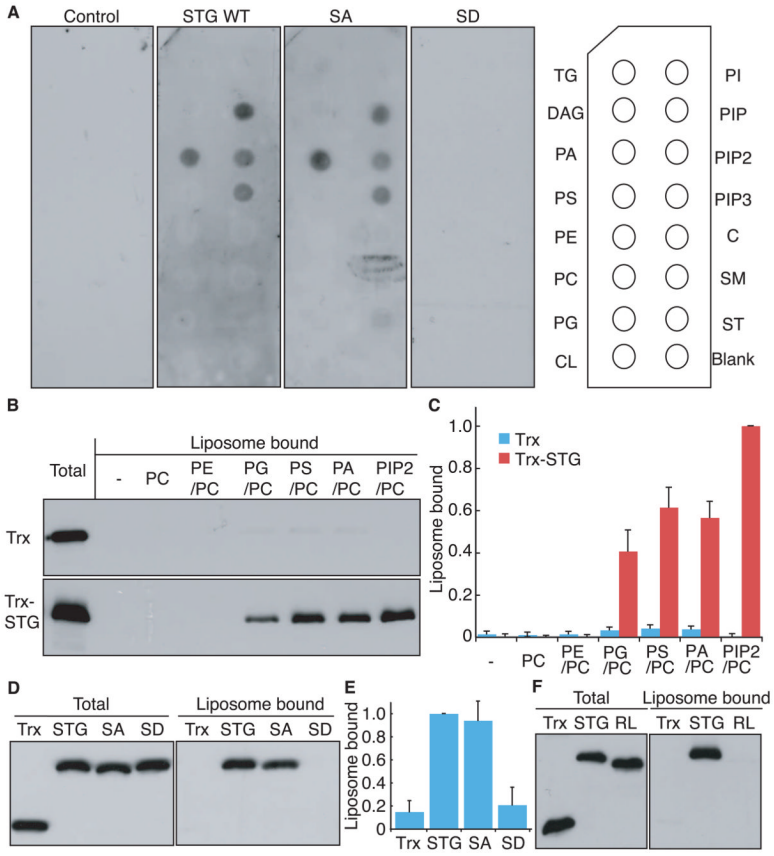

Figure 3. Stargazin binds negatively-charged lipids in a phosphorylation-dependent manner

(A) The cytoplasmic domain of stargazin (STG) binds directly to phosphatidic acid (PA) and phosphoinositides (PIP, PIP_2, PIP_3). GST-fused stargazin cytoplasmic domains were overlaid on a membrane spotted with various lipids and bound stargazin was detected with anti-GST antibody. TG, triglyceride; DAG, diacylglycerol; PA, phosphatidic acid; PS, phosphatidylserine; PE, phosphatidylethanolamine; PC, phosphatidylcholine; PG, phosphatidylglycerol; CL, cardiolipin; PI, phosphatidylinositol; PIP, phosphatidylinositol 4-phosphate; PIP_2, phosphatidylinositol 4,5-biphosphate; PIP_3, phosphatidylinositol 3,4,5-triphosphate; C, cholesterol; SM, sphingomyelin; and ST, 3-sulfogalactosylceramide. (B) The cytoplasmic domain of stargazin recognizes negatively-charged liposomes. Thioredoxin (Trx)-fused stargazin cytoplasmic domains were mixed with liposomes containing phosphatidyl choline (PC) and various lipids (9:1). Subsequently, liposome-bound and unbound proteins were separated by sucrose gradient centrifugation and examined by western blotting. (C) Quantitation of liposome-bound proteins normalized against PIP_2/PC-binding stargazin. (D) The cytoplasmic domain of stargazin interacts with PC/PA liposomes in a phosphorylation-dependent manner. PC/PA liposomes interact with thioredoxin-fused cytoplasmic domains of stargazin and stargazin^{SA}, but not stargazin^{SD}. (E) Quantitation of liposome-bound proteins normalized against stargazin. (F) The cytoplasmic domain of stargazin interacted with PC/PA liposomes via its positively charged residues (arginines). Eight of the arginine residues located around the stargazin phosphorylation sites and all arginine residues were replaced with seven leucines and one glycine residue (RL). PC/PA liposomes interacted with the thioredoxin-fused cytoplasmic domain of stargazin (STG), but not stargazin^{RL}, which indicates that the cytoplasmic domain of stargazin interacted with lipid bilayers via an electrostatic interaction. Error bars in (C) (n = 3) and (E) (n = 5) show means ± SEM.

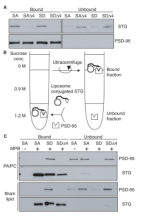

Figure 4. Lipid bilayers inhibit binding of stargazin to PSD-95

(**A**) In the absence of lipids, the four C-terminal amino acids of stargazin^{SD} (SD) and stargazin^{SA} (SA) bind PSD-95. The PSD-95 PDZ domain-bound and unbound stargazin (STG) cytoplasmic domains were separated with glutathione beads. Both stargazin^{SD} and stargazin^{SA} bound to the PDZ domain, whereas mutants lacking the last four amino acids (Δ4) did not bind. (B) This diagram shows the experimental scheme to examine the effects of lipid bilayers on the stargazin binding to PSD-95. Liposomes conjugated to the stargazin cytoplasmic domain were incubated with the PSD-95 PDZ domains. Stargazin-bound and unbound PSD-95 were separated by sucrose gradient centrifugation. (**C**) Lipid bilayers inhibit stargazin interaction with PSD-95. Stargazin did not conjugate with liposomes lacking MPB-PE (MPB). The PSD-95 PDZ domains bound liposomes conjugated with stargazin^{SD} but not stargazin^{SA} or stargazin^{SD}Δ4. Liposomes constituted with PC/PA or brain lipids showed similar results.

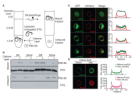

Figure 5. PSD-95 binding requires stargazin dissociation from lipid bilayers

The cationic lipid lipofectamine increased the interaction between stargazin^{SA} (SA) and PSD-95. (A) Shown is the experimental scheme for examining the effects of cationic lipids on stargazin (STG) binding to PSD-95. Lipofectamine (approx. 100 μM) was added to a stargazin-conjugated liposome and PSD-95 mixture. Stargazin-bound and unbound PSD-95 were separated by sucrose gradient centrifugation. (B) PSD-95 did not bind stargazin^{SA} in the phosphatidylcholine/phosphatidic acid liposomes. Upon addition of lipofectamine, PSD-95 bound the stargazin^{SA} from liposomes but not the stargazin^{SA}Δ4. The interaction between the stargazin^{SD}-containing liposomes and PSD-95 was unaltered by lipofectamine. Notably, the weak signal observed for the stargazin^{SA} Δ4 was also observed in liposomes conjugated with cysteine alone, which suggests that this weak signal is non-specific (Figure S5). (C) The cytoplasmic domain of stargazin localized at the plasma membrane in a phosphorylation-dependent manner. The cytoplasmic domains of stargazin and mutants were tagged with a myristoylation motif at the N terminus, to mimic the localization of the cytoplasmic domain near a transmembrane domain in stargazin, and with GFP at the C terminus, to monitor its distribution (myrSTG), and expressed in CHO cells together with mCherry-tagged R-Pre, which interacts with negatively charged membranes (C). The myristoylated stargazin^{SA} mutant (myrSA) colocalized with mCherry-R-pre, whereas GFP alone, myrSD, and myrSTG did not. The relative distribution of stargazin was analyzed relative to that of mCherry-R-Pre. (D) The cationic lipid sphingosine translocated myrSA from the plasma membrane to the cytoplasm, similarly to R-pre. Addition of the cationic lipid sphingosine (100 μM for 5–20 min) induced the relocalization of myrSA from the plasma membrane to the cytoplasm. The relative distribution of stargazin and R-pre was shown after adjustment of total amount of signal from single cell as 1 because total amount of proteins were not changed before and after addition of cationic lipid. All data are shown as means ± SEM (n = 10 cells).

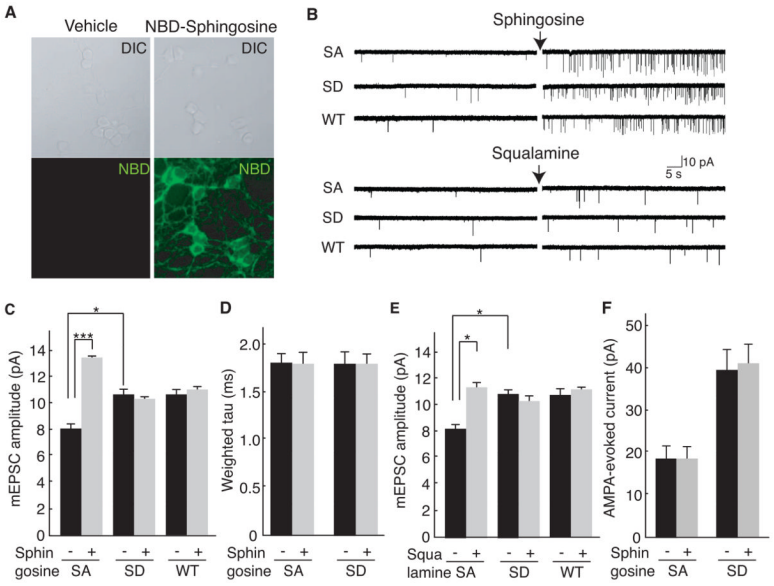

Figure 6. Cationic lipids enhance synaptic activity of AMPA receptors in a stargazin phosphorylation-dependent manner

(A) The cationic lipid sphingosine-NBD inserts into neuronal membranes. Sphingosine-NBD (2.5 μM) or vehicle (ethanol) was added to cerebellar granule cells and analyzed by confocal microscopy. Top panels, DIC; Bottom panels, NBD channel. (B–D) AMPA receptor-mediated miniature EPSCs (mEPSC) were recorded from cerebellar granule cells from stargazin^{SA} (SA), stargazin^{SD} (SD) and wild-type mice (WT) before and after addition of cationic lipids, sphingosine (2.5 μM) or squalamine (2.5 μM). Shown are the representative traces (B), mean amplitude (C), and weighted tau (D) of AMPA receptor-mediated mEPSC from each genotype before and after sphingosine addition. In Stargazin^{SA} mice, the amplitude of mEPSC increased upon addition of sphingosine, but no changes in decay kinetics were observed. No similar increase in amplitude was observed for WT and Stargazin^{SD} mice (n = 164–188 and 1626–1869 events from 13–15 cells for each genotype before and after sphingosine treatment, respectively). *** P<0.005. (E) Mean amplitude of AMPA receptor-mediated mEPSC from each genotype before and after squalamine addition (2.5 μM) (n = 48 (before squalamine) and n = 169 (after squalamine) events from six stargazin^{SA} cells; n = 49 (before squalamine) and n = 160 (after squalamine) events from seven stargazin^{SD} cells.). * $P < 0.01$. (F) AMPA-evoked currents did not change upon addition of sphingosine (n = 13–15 cells for each genotype before and after sphingosine treatment, respectively). Data are shown as means ± SEM.

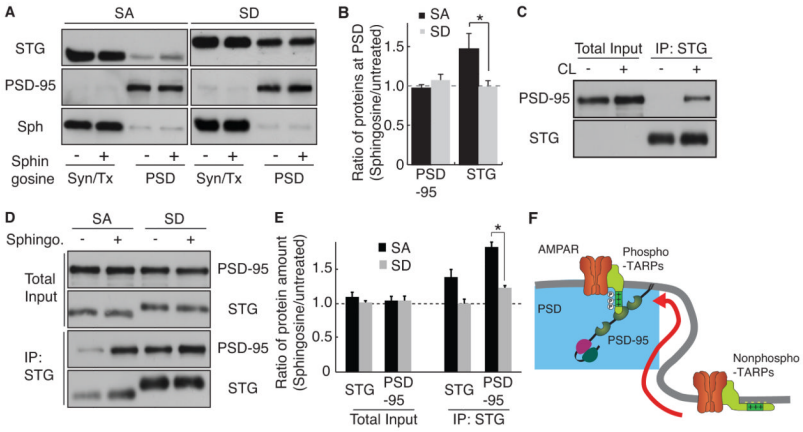

Figure 7. Cationic lipids enhance translocation of stargazin to synapses in a stargazin phosphorylation-dependent manner

(A and B) Treatment with a cationic lipid increased the synaptic expression of stargazin^{SA}, but not of stargazin^{SD}, without changes in the synaptic expression of PSD-95. Cerebellar granule cells from stargazin^{SA} and stargazin^{SD} mice were treated with and without sphingosine (10 μM for 5 min), which was followed by fractionation of soluble Triton X-100 (Syn/Tx) and insoluble PSD-enriched (PSD) fractions. Stargazin (STG) translocated into the PSD fraction after addition of sphingosine in neurons from stargazin^{SA}, but not stargazin^{SD}, mice, without changes in PSD-95 and synaptophysin (Sph). Protein amounts were quantitated using ImageJ. Data are shown as means ± SEM (n = 6). (C) Stargazin immunoprecipitated PSD-95 from cerebellar granule cells treated with a crosslinker (CL), which indicated that stargazin did not interact artificially with PSD-95 during incubation (in test tubes) under this experimental condition. (D) Cationic lipid treatment (10 μM sphingosine 5 min with 2 μM TTX) increased the interaction between PSD-95 and Stargazin^{SA}, but not Stargazin^{SD}, without changes in the total levels of protein expression. (E) Quantitative analyses showed that total protein expression was no significantly different after the treatment with cationic lipids, whereas the level of PSD-95 immunoprecipitated with the anti-stargazin antibody was significantly increased. Data are shown as means ± SEM (n = 3). *; $P < 0.01$. (F) A model for the TARP phosphorylation-mediated regulation of synaptic AMPA receptors via lipid bilayers. The interaction of negatively charged lipid bilayers with stargazin inhibits the binding of stargazin to PSD-95. Dissociation of lipids from phosphorylated stargazin leads to its binding to PSD-95 at synapses.